

Supporting Information

Room-Temperature Ferroelectricity and Switchable Diode Effect in Two-Dimensional α -In₂Se₃ Thin Layers

Siyuan Wan¹, Yue Li¹, Wei Li², Xiaoyu Mao¹, Wenguang Zhu^{1,2,*} & Hualing Zeng^{1,2,*}

¹International Center for Quantum Design of Functional Materials (ICQD), Hefei National Laboratory for Physical Science at the Microscale, and Synergetic Innovation Center of Quantum Information and Quantum Physics, University of Science and Technology of China, Hefei, Anhui 230026, China

²Key Laboratory of Strongly-Coupled Quantum Matter Physics, Chinese Academy of Sciences, Department of Physics, University of Science and Technology of China, Hefei, Anhui 230026, China

* Corresponding author

E-mail: wgzhu@ustc.edu.cn; hlzeng@ustc.edu.cn

Supplementary Note 1: Stripe domain structure in α -In₂Se₃ thin layers

The ferroelectric domain structure was characterized by PFM. An obvious 180° stripe domain pattern has been found in ~20nm α -In₂Se₃ as shown in Figure S1. The stripe domain structure was observed in a scan area of 8×8μm². To ensure the reliability of the observation, we scanned a zoom in area with higher spatial resolution and changed the scanning angle in the PFM measurements. We found there was no difference between the two measurements. The domain structures were self-consistent in the two PFM images, which proved the robustness of periodic ferroelectric domains in α -In₂Se₃ thin layers.

Supplementary Note 2: the electric polarization dependence on layer thickness in α -In₂Se₃ thin layer

We studied the electric polarization dependence on layer thickness in α -In₂Se₃ thin layer. In conventional bulk ferroelectrics, the piezoresponse is expected to be enlarged with increasing sample volume due to the accumulation of polarization in same orientation. However, for α -In₂Se₃ thin layers, we observed that their net polarization was independent of sample thickness. In figure S3, we show the PFM measurements on different layers. Ferroelectric domains were directly visualized with contrasted piezoresponse signal intensity in Figure S3a. In Figure S3b, the PFM amplitude as a function of layer thickness was summarized. By in situ comparing the layer thickness and the PFM amplitude intensity, we found there was no correlation between the two. The strongest piezoresponse signal was observed from the thinnest layer with 5nm thickness. For a given QL, owing to the presence of out-of-plane electric polarization, there is strong built-in electric field within the layer, with positive polarization charges on one side and negative polarization charges on the other side. In few layer α -In₂Se₃ with thickness above 2 QLs, as pointed out in previous theoretical study, the electric dipole in all the QLs preferred to align in the same orientation. The neighboring layers are stacked together with opposite charged sides, resulting strong charge transfer between layers. The charge transfer will significantly reduce the polarization induced built-in electric field within the material. Thereby, the net electric polarization in α -In₂Se₃ thin layer (>2QLs) tends to be saturated, leading sample thickness independent piezoelectric response. Other possible reason for the observed thickness independent electric polarization may lie in the coexistence of non-alpha phase In₂Se₃ thin layers, which may dilute the measured PFM amplitude as not all the layers have contributions to the piezoresponse signal.

In Figure S3c, we show the resonance spectrum of the cantilever used in the PFM measurement. The quality factor of the resonance was defined by $Q = \Delta f/f_0$. The quality factor was used to estimate the longitudinal piezoelectric coefficient d_{33} of α -In₂Se₃ films

Supplementary Note 3: Schottky barrier formation in α -In₂Se₃/graphene heterostructure based ferroelectric diode

For n-type semiconductor α -In₂Se₃, the band gap E_g is around 1.4eV¹⁻³, with its electron affinity at around 3.6eV.⁴ The work function of the top/bottom electrodes were taken as 4.6eV⁵ (intrinsic graphene) and Al (4.33eV). At graphene/ α -In₂Se₃ interface, electrons in α -In₂Se₃ would move spontaneously into graphene due to a higher Fermi level. Therefore, positive holes would accumulate at the interface and generate a Schottky barrier. For the graphene samples used in our study, we found the monolayer graphene was p-type while few layer graphene (FLG) was intrinsic. Thereby, in FLG/ α -In₂Se₃/graphene ferroelectric diode, the Schottky barrier at the two interfaces, FLG/ α -In₂Se₃ and graphene/ α -In₂Se₃, were with different heights. The Schottky barrier at FLG/ α -In₂Se₃ interface was lower than that at graphene/ α -In₂Se₃ interface. The same phenomenon occurred in the metal/ α -In₂Se₃/graphene ferroelectric diode. The α -In₂Se₃/Ti(Al) interface was with a lower barrier than that of graphene/ α -In₂Se₃ interface.

Supplementary Note 4: Switchable rectifying behavior in metal/ α -In₂Se₃/graphene ferroelectric diode

As a test of the interface effect on the polarization stability of α -In₂Se₃, we changed the top electrode material in the

ferroelectric diode from few layer graphene to metal Al. It is well understood that the metal electrode would significantly reduce the electric polarization of a given ferroelectric due to its finite electron screen length. In our metal/ α -In₂Se₃/graphene ferroelectric diode, we observed similar electric transport properties with worse performance as shown in Figure S7. The polarity of the diode could be switched under a higher DC bias ± 4 V (Figure S7c,d). The I-V curves in Figure S7g,h show characteristic hysteresis behavior, but with less resistive switching effect if compared to that in the FLG/ α -In₂Se₃/graphene ferroelectric diode. The observed electric transport behavior can be explained within the same scenario as discussed in the main text, the different modification of the Schottky barrier at the two interfaces (metal/ α -In₂Se₃ and graphene/ α -In₂Se₃) by the two reversed electric polarizations. We found the on/off ratio of the metal/ α -In₂Se₃/graphene ferroelectric diode was at the order of $\sim 10^4$. The study on the interface effect indicates the robustness and stability of the 2D ferroelectricity in α -In₂Se₃.

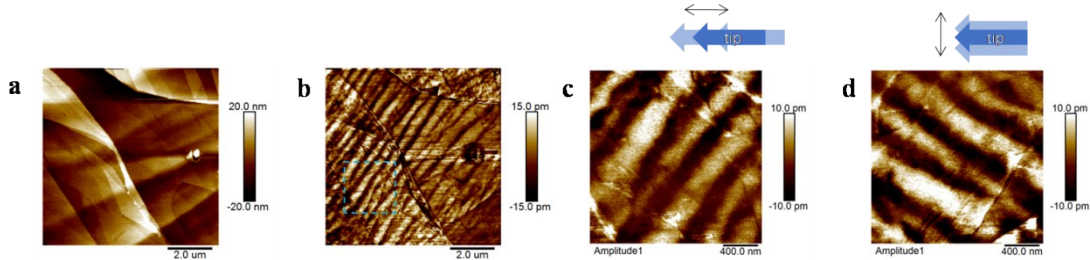


Figure S1. Stripe domains of α -In₂Se₃ thin layers on heavily doped Si substrate. a) Topography and b) corresponding PFM amplitude images. The scale bar is 2 μ m. c), d) PFM amplitude images of a zoom-in area denoted by a dash-lined frame in b) with different scanning directions. The scale bar is 400 nm. The tip scanning directions in c) and d) are in-plane rotated 90° relative to each other, as illuminated by the cartoon.

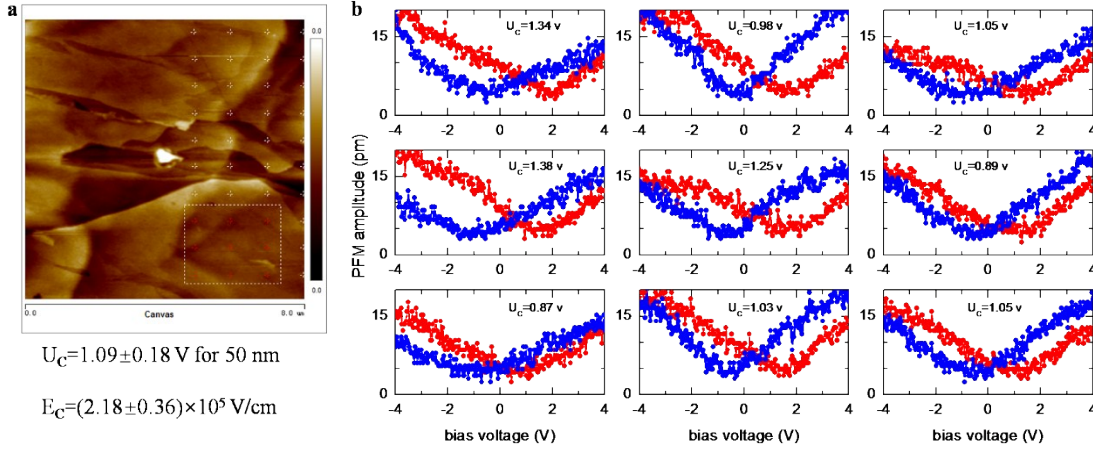


Figure S2. a) Topography images of α -In₂Se₃ thin layers. Red points denote the location of each single polling measurement. b) The corresponding PFM amplitude hysteresis loops as a function of applied bias voltage. The coercive field of 50nm α -In₂Se₃ was estimated by an average of the extremes in these PFM amplitude spectra.

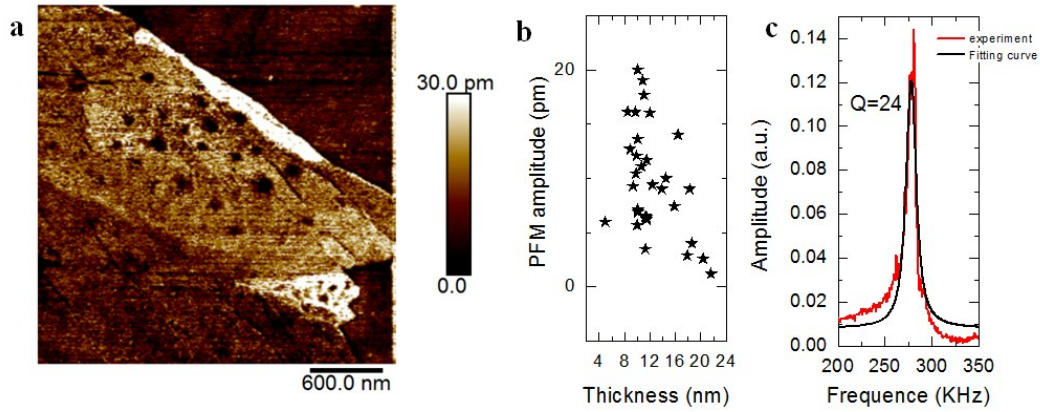


Figure S3. PFM amplitude as a function of α - In_2Se_3 thickness a) PFM amplitude images ($3 \times 3 \mu\text{m}^2$) of α - In_2Se_3 thin layers on heavily doped Si substrate. The scale bar is 600 nm. b) PFM amplitude dependence on the thickness of α - In_2Se_3 thin layer in a). The thinnest ferroelectric α - In_2Se_3 thin layer is with film thickness down to 5 nm. c) The vibrational amplitude of the cantilever versus with the frequency of the applied ac voltage (1V) in PFM measurement with contact mode. Red line is experimental data. Black line is Lorentz fitting. The quality factor Q of the resonance is 24.

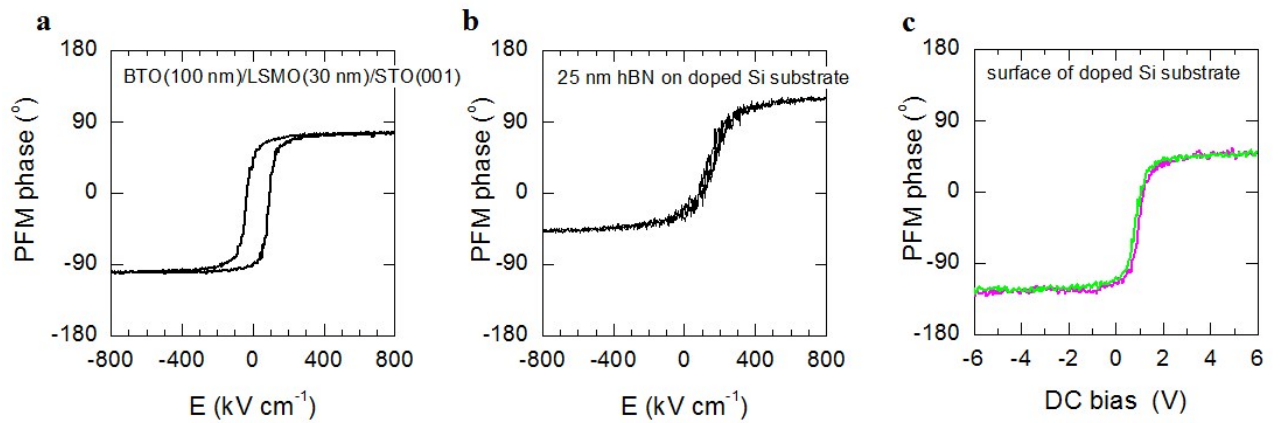


Figure S4. The out-of-plane phase response as a function of tip bias measured from a) $\text{BaTiO}_3(100\text{nm})/\text{La}_{0.7}\text{Sr}_{0.3}\text{MnO}_3(30\text{nm})/\text{SrTiO}_3$ sample, b) hBN(25nm)/doped Si sample, and c) heavily doped Si substrate. Clear hysteric loop can be observed only in ferroelectric BaTiO_3 sample.

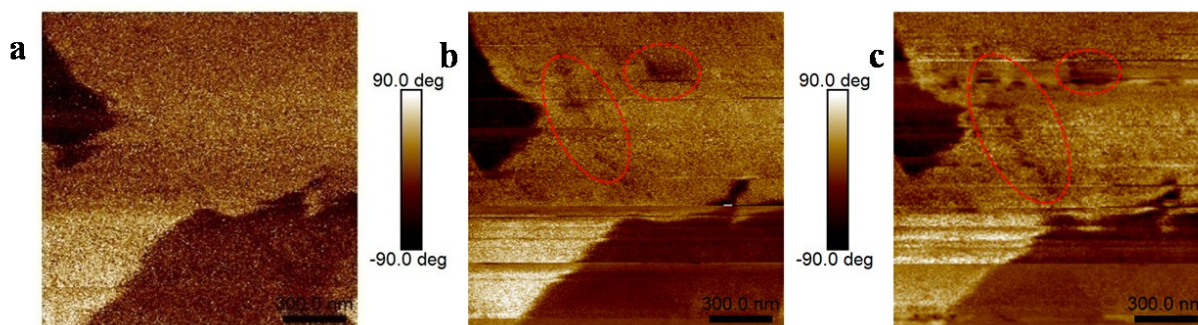


Figure S5. Evolution of ferroelectric domains. Out-of-plane PFM phase images of α - In_2Se_3 thin layers with tip bias at a) 1V, b) 1.5V and c) 2V. The scale bar is 300 nm. When increasing the driving tip bias in PFM measurements, the direction of ferroelectric domain is gradually flipped, resulting a growth of domain (as marked by the red dash circles) in antiparallel direction.

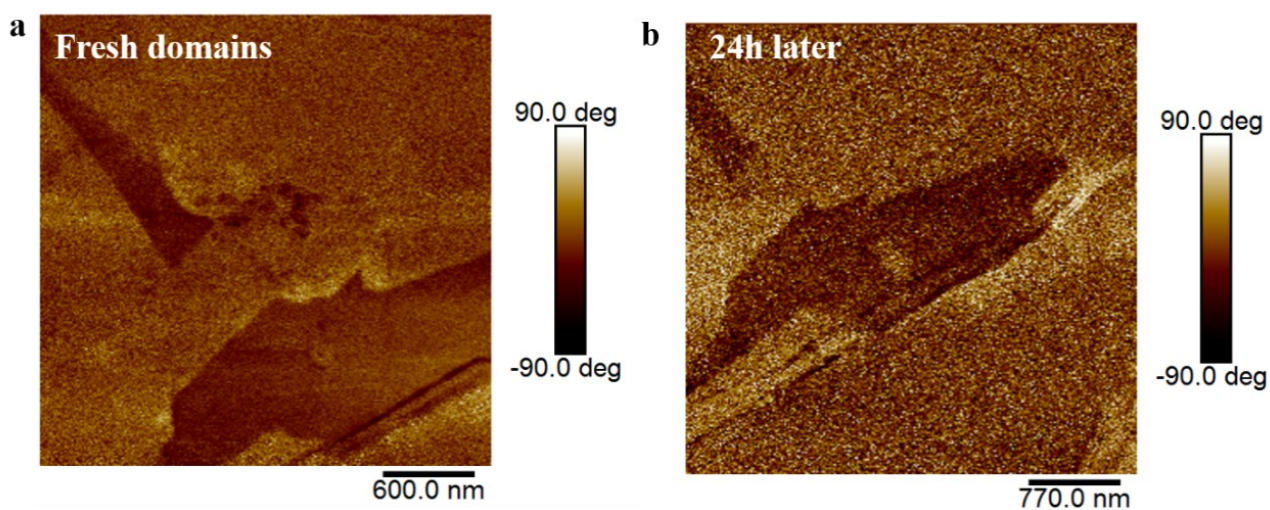


Figure S6. Stability of ferroelectric domains. PFM Out-of-plane phase images measured from a) a fresh α - In_2Se_3 thin layers and b) the same area after 24h.

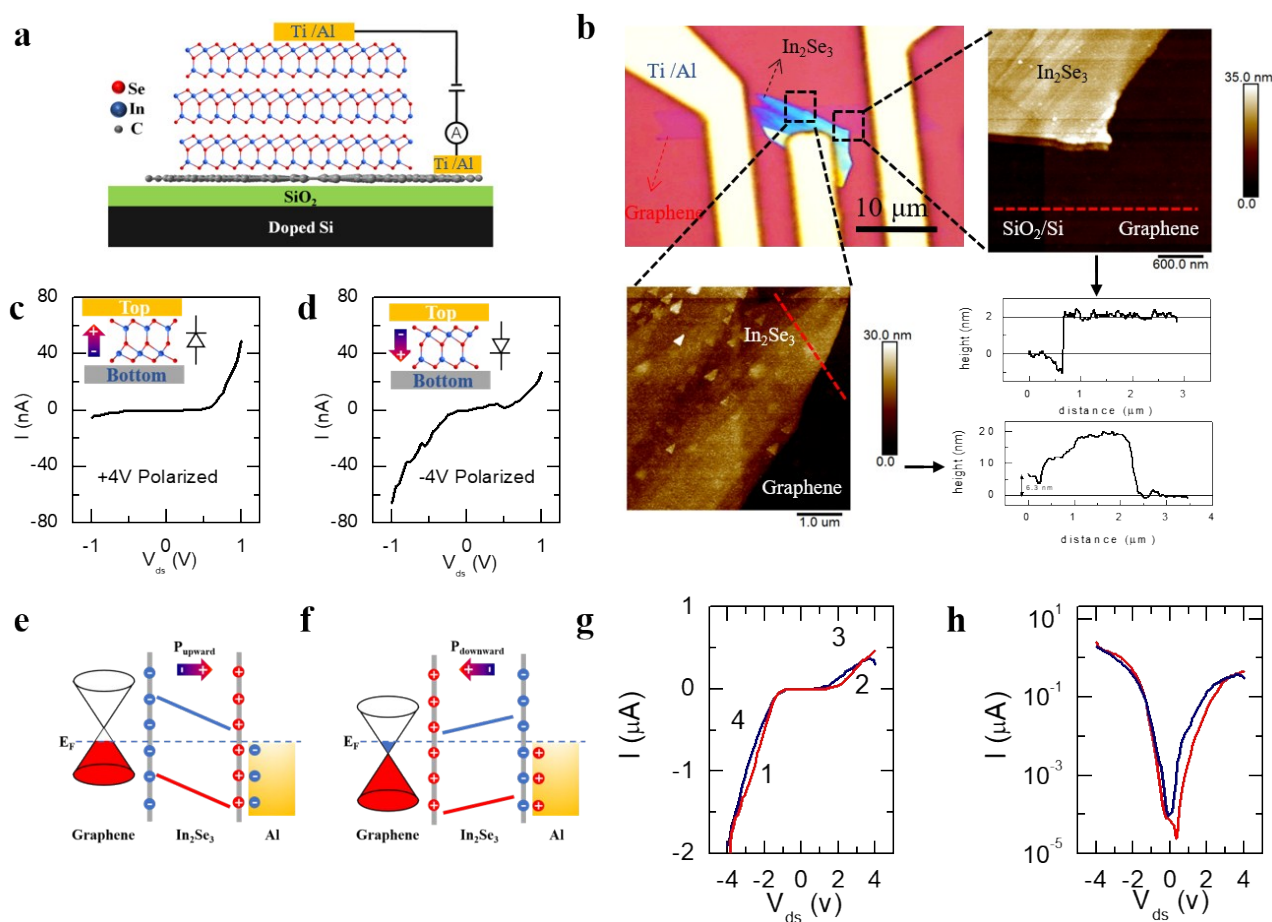


Figure S7. Switchable ferroelectric diode based with metal/ α -In₂Se₃/graphene structure. a) Schematic and b) optical image of the device. The AFM topography measurements show that the thinnest region of α -In₂Se₃ is 6.3 nm and the bottom graphene electrode used in the device is bilayer, which can be seen from the corresponding height profiles taken along the red dash line. c) and d) I-V curves of ferroelectric diode with switchable rectifying behavior. e) and f) Schematic of energy band diagrams of graphene/In₂Se₃ heterostructure, illustrating the evolutions of Schottky barrier on the polarization state of the ferroelectric. The positive and negative charges on vertical grey lines stand for the polarization charges at the top and bottom sides of α -In₂Se₃ thin layer. The screening charges are visualized in the metal electrode. g) I-V curves measured under high DC bias, showing clear hysteresis characteristics. The numbers indicate the voltage sweeping sequence. h) The same I-V curves under high DC bias on semilogarithmic scales.

Reference:

1. Q. Wang, L. Yang, S. Zhou, X. Ye, Z. Wang, W. Zhu, M. D. McCluskey and Y. Gu, *J. Phys. Chem. Lett.*, 2017, 8, 2887-2894.
2. W. Ding, J. Zhu, Z. Wang, Y. Gao, D. Xiao, Y. Gu, Z. Zhang and W. Zhu, *Nat. Commun.*, 2017, 8, 14956.
3. Jacobs-Gedrim R B, Jacobs-Gedrim, Shanmugam M, G. R. B. Jain N, Shanmugam M and J. N, *ACS Nano*, 2013, 8, 514-521.
4. S. I. Drapak, Kovalyuk, Z. D., Netyaga, V. V., & Orletskii, V. B., *Tech. Phys. Lett.*, 2002, 28, 707–710.
5. Y.-J. Yu, Y. Zhao, S. Ryu, L. E. Brus, K. S. Kim and P. Kim, *Nano Lett.*, 2009, c 9, 3430-3434.